NJC

Accepted Manuscript

This is an *Accepted Manuscript*, which has been through the Royal Society of Chemistry peer review process and has been accepted for publication.

Accepted Manuscripts are published online shortly after acceptance, before technical editing, formatting and proof reading. Using this free service, authors can make their results available to the community, in citable form, before we publish the edited article. We will replace this *Accepted Manuscript* with the edited and formatted *Advance Article* as soon as it is available.

You can find more information about *Accepted Manuscripts* in the Information for Authors.

Please note that technical editing may introduce minor changes to the text and/or graphics, which may alter content. The journal's standard Terms & Conditions and the Ethical guidelines still apply. In no event shall the Royal Society of Chemistry be held responsible for any errors or omissions in this *Accepted Manuscript* or any consequences arising from the use of any information it contains.

ROYAL SOCIETY OF CHEMISTRY

www.rsc.org/njc

TOC: Co_3O_4 nanosheet arrays grown on carbon cloth homogeneously, excellent electrochemical performance was obtained due to the unique structure and morphology.

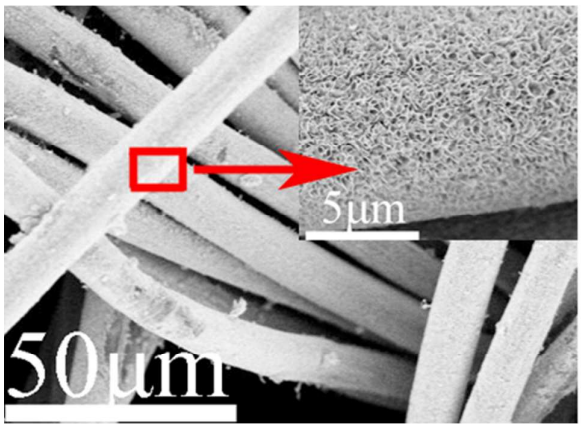

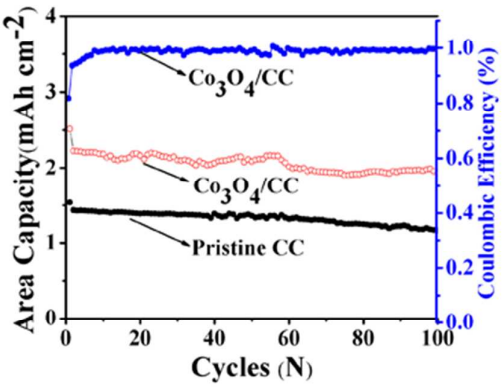

NJC

RSCPublishing

LETTER

Hierarchical porous Co_3O_4 nanosheet arrays directly grown on carbon cloth by an electrochemical route for high performance Li-ion batteries

Cite this: DOI: 10.1039/c3nj00000x

Received 00th XXXXX 2013,
Accepted 00th XXXXX 2013

DOI: 10.1039/c3nj00000x

www.rsc.org/njc

Chao Cheng[1a], Gang Zhou[1a], Jun Du[a], Haiming Zhang[a], Di Guo[a], Qiuhong Li[a], Weifeng Wei[b] and Libao Chen*[a]

Co_3O_4 nanosheet arrays (NSAs) were successfully grown on flexible carbon cloth (CC) by a simple electrochemical deposition method. The deposited films were composed of homogeneous ultrathin hierarchical porous Co_3O_4 nanosheets. Such Co_3O_4 NSAs/CC electrode showed superior electrochemical performance, indicating a promising method to fabricate flexible electrode for Li-ion batteries.

During the past two decades, Li-ion batteries have been widely used in portable electronic devices and electric vehicles due to the high power density and long cycle life.[1,2] Though the graphite has been commercialized as anode electrode, the low theoretical capacity (372 mAh g^{-1}) limits its application in high energy density batteries. Compared with graphite, Cobalt-based oxides present larger specific capacity. [3-8] Thus many researchers paid attention to the transition-metal oxides, such as Co_3O_4, $CuCo_2O_4$,[6] $NiCo_2O_4$[7] and $ZnCo_2O_4$.[8] Among them, Co_3O_4(theoretical capacity 890 mAh g^{-1}) has been intensively investigated as candidate for graphite negative electrodes. As the morphology and particle size play an important role in the performance of the materials, great efforts have been paid to obtain Co_3O_4 with different nanostructures. Reddy synthesized Co_3O_4 compounds using different molten salts and studied their morphology and Li-storage properties.[9,10] Shim et al. prepared porous Co_3O_4 hollow rods through a biomineralization process.[11] Those Co_3O_4 nanostructures have exhibited an excellent reversible specific capacity of 903 mAh g^{-1} after 20 cycles. Hwang et al. synthesized uniform hexagonal-shaped cobalt oxide nanodisks in large scale via a hydrothermal process.[12] The electrode showed an initial lithium insertion capacity of 2039 mAh g^{-1}. Other methods were also used to prepare Co_3O_4 nanostructures, such as template methods,[13] electrodeposition[14]and chemical vapor deposition.[15] However, some problems still exist as summarized in recent reviews,[16] such as the structure changed during the cycling performance, which will lead the capacity decrease. Until now neither the rate capacity nor the cycling stability has achieved our desiring.

Among the methods to prepare Co_3O_4 nanostructures, those directly growing on current collector is a promising strategy to construct a stable electrode with large specific area and good conductivity. Chen's group has prepared cobalt oxide nanowire arrays films on large-area metallic substrates.[17,18] The Co_3O_4 nanowire arrays have been shown a very small capacity fading of 0.13% per cycle. Both Chou and Yen's groups have obtained Co_3O_4 thin film on the stainless steel substrates.[19,20] Compared with the substrates such as Ti foil and Ni foam, CC has better properties on lightweight and stability. Furthermore, it can make a contribution to the capacity of the anode, which will increase the energy density and power density of the whole battery. In this paper, we reported a simple electrochemical deposition route to obtain Co_3O_4 NSAs/CC flexible electrode with hierarchical porous structure. The Co_3O_4 NSAs/CC showed superior electrochemical performances, which made it to be a more promising alternative anode material for Li-ion batteries.

Fig.1 shows the XRD pattern of the as-prepared sample. All the diffraction peaks can be indexed to the cubic phase of Co_3O_4 except for the peak arising from the CC substrate at about 24°, which is consistent with the standard spectrum (JCPDS file no. 42-1467).

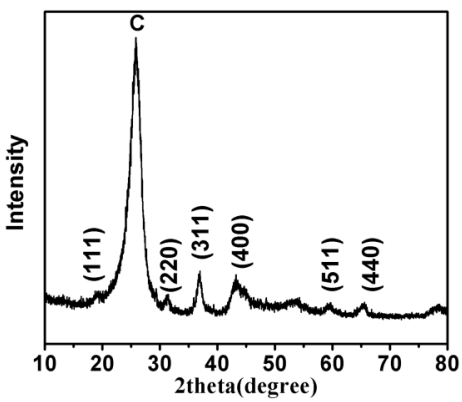

Fig. 1 XRD pattern of the Co_3O_4 NSAs/CC

Fig.2a, b and c show the low- magnification and high-magnification SEM images of the Co_3O_4 NSAs/CC. It can be clearly seen that the uniform Co_3O_4 nanosheet arrays are well aligned on CC, which are interconnected each other. Fig. 2d provides a cross-section SEM picture of the single Co_3O_4 NSAs/CC. It can clearly see the unique core/shell structure, the Co_3O_4 nanosheet shells cover the CC core.

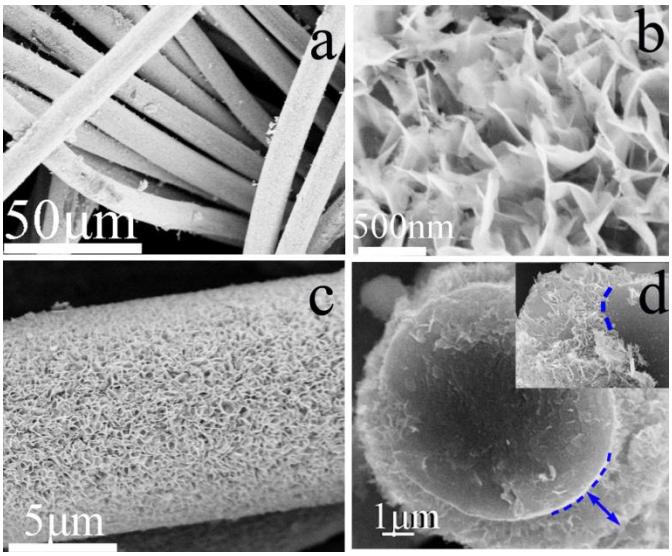

Fig. 2 (a, b, and c) SEM images of the Co_3O_4 NSAs/CC; (d) and the upper right inserts in (d) correspond to the side views of the Co_3O_4 NSAs/CC.

Further characterization for Co_3O_4 nanostructures was performed with TEM. It was shown in Fig. 3a and b that Co_3O_4 nanosheets are composed of many nanoparticles (about 10 nm in size) and nanopores. The interconnected and porous nanosheets construct the hierarchical porous structure of the electrode. The corresponding HRTEM image (Fig. 3 c) indicates that aligned lattice fringes with the spacing of 0.284 nm corresponds to the (2 2 0) plane of cubic Co_3O_4, which is consistent with the XRD results. The SAED rings can also be indexed to the cubic Co_3O_4 phase (Fig. 3 d).

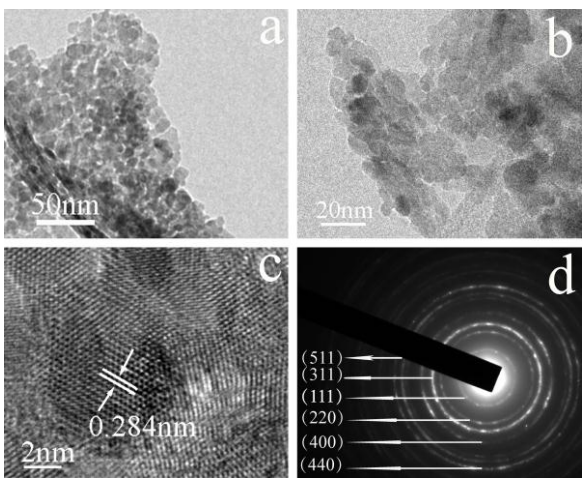

Fig.3 (a, b) TEM images; (c) HRTEM image; (d) SAED pattern of the as-prepared Co_3O_4 nanosheets

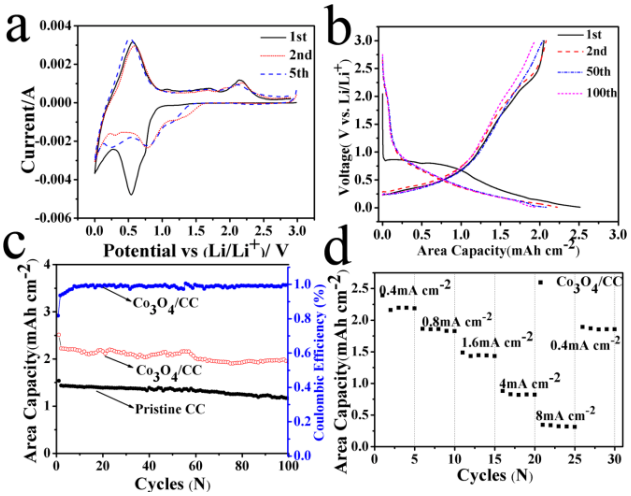

Fig. 4 (a) Typical CV curves of Co_3O_4 NSAs/CC; (b) Galvanostatic charge-discharge curves of Co_3O_4 NSAs/CC electrode; (c) Cycling performance and coulombic efficiency of pure CC and Co_3O_4 NSAs/CC at the current density of 0.4 mA cm^{-2}; (d) The charge-discharge rate performances of Co_3O_4 NSAs/CC at various current.

The CV curves of as-prepared Co_3O_4 NSAs/CC anodes were tested at a scan rate of 0.5 mV s^{-1} in the voltage range 0.01–3V at room temperature, as shown in Fig. 4 a. In the first cathodic process, there is an intense peak located at around 0.55 V, which is corresponded to the electrochemical reduction reaction of Co_3O_4 to metallic Co and formation of SEI layer. In the subsequent two scans, the CV curves show two cathodic peaks at ~0.22V and ~0.77V which are generally attributed to the reaction of Co(III) to Co(II) and metal Co. The cathodic peaks at ~0V is related to lithium insertion into CC.[21,22] In the anodic process, the oxidation peak at 2.1V corresponds to the decomposition of Li_2O and the formation of Co_3O_4. And the other oxidation peak at 0.56V is related to the lithium ion extraction from CC. The electrochemical reactions are the same as the early reports.[11,23]

Fig. 4 b shows the galvanostatic charge-discharge curves of the Co_3O_4 NSAs/CC electrode in the 1st, 2nd, 50th and 100th cycles between 3 and 0.01 V (vs Li^+/Li) at a current density of 0.4 mA cm^{-2}. The first discharge and charge capacities are 2.51 mAh cm^{-2} and 2.06 mAh cm^{-2} with a high coulombic efficiency of 82.1%. The irreversible capacity may be resulted from irreversible lithium-ion loss due to the electrolyte decomposition and the formation of a SEI layer.[24]In the first discharge curve, it is clearly to see that a long plateau is located at 0.8 V, then decreases slowly to 0.01V. The discharge capacities of Co_3O_4 NSAs/CC electrode in the 2nd, 50th and 100th are 2.22, 2.08, 1.94mAh cm^{-2}. According to the weight percentage of Co_3O_4 in the total composite electrode, the specific capacity of Co_3O_4 nanosheets can be calculated as follows:

$$C=C_{Co3O4}\times\text{mass percentage of } Co_3O_4+ C_{CC} \times\text{mass percentage of CC}$$

Where C_{Co3O4} is the capacity of Co_3O_4, C_{CC} is the capacity of CC. The area density of Co_3O_4 is 0.8 mg cm^{-2} and presents more than 787

mAh g^{-1} during the 100 cycles at the current of 0.4 mA cm^{-2}. The area density of CC is 14.3 mg cm^{-2} and present 90 mAh g^{-1} at the current of 0.4 mA cm^{-2}. Except the capacity of CC, the capacities of Co_3O_4 NSAs are 0.97, 0.79, 0.78, 0.63 mAh cm^{-2} at a current of 0.4 mA cm^{-2} in the 1st, 2nd, 50th and 100th. Correspondingly, the weight specific capacities of Co_3O_4 NSAs are 1200, 987, 975, 787mAh g^{-1} in the 1st, 2nd, 50th and 100th cycles, which is better than the Ref. 25.

The cycling behavior and coulombic efficiency of pristine CC and Co_3O_4 NSAs/CC are shown in Fig. 4 c at a rate of 0.4 mA cm^{-2}. During the 100 cycles, the pristine CC shows good capacity retention. It can be found that the CC makes a significant contribution to the total capacity of the electrode. Compared with the pristine CC, the Co_3O_4 NSAs/CC exhibits much higher area capacity. The reversible capacity is 2.06 mAh cm^{-2} in the first cycle, and maintain above 1.94 mAh cm^{-2} after 100 cycles. This demonstrates that the Co_3O_4 NSAs/CC exhibits excellent cycling performance. In the initial 16 discharge/charge cycles, the coulombic efficiency rises from 82.1% to 98.7%. Then it is kept close to 100% in the following cycles. The rate capability of Co_3O_4 NSAs/CC was evaluated at different discharge-charge current in the voltage range of 0.01 to 3.0 V, as shown in Fig. 4 d. The area capacity of the Co_3O_4 NSAs/CC are 1.85, 1.43, 0.82, 0.34 mAh cm^{-2} at the current density of 0.8, 1.6, 4, 8 mA cm^{-2}, which means the Co_3O_4 NSAs present 740, 583, 380 and 160 mAh g^{-1}at the various current. It should be noted that even at the rate as high as 8 mA cm^{-2}, the Co_3O_4 NSAs/CC still can deliver a capacity of 0.34 mAh cm^{-2}, indicating the high rate capability.

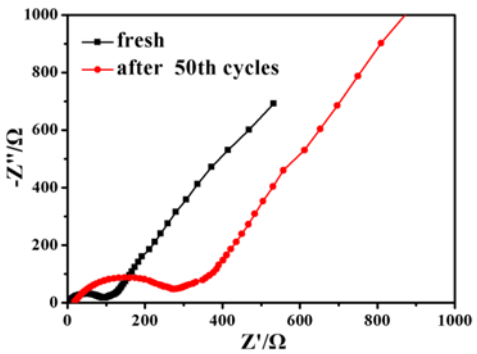

Fig.5 Electrochemical impedance spectras for the Co_3O_4 NSAs/CC.

The characteristic EIS curves (Nyquist plots) of Co_3O_4 NSAs/CC are shown in Figure 5. Both plots exhibit a semicircle in the high frequency region and a sloped line in the low frequency region. Compared with the conventional binder-enriched electrode,[26] the fresh electrode we obtained shows a smaller semicircle. It may be due to the active material directly grown on the current collector without any binder, which will shorten the electron transport distance. The 50-cycled electrode has a larger semicircle, which may be due to the formation of SEI during the cycles. This impedance evolution can well match the electrochemical performance of the electrode. The superior electrochemical performance of Co_3O_4 NSAs/CC is due to the following reasons: 1) because the ultrathin Co_3O_4 nanosheets are composed of small particles and pores, this microstructure can buffer the volume effect of Co_3O_4 nanoparticles during the intercalation/de-intercalation reaction; 2) the porous structure between the interconnected nanosheets and the nanopores on the Co_3O_4 nanosheets can facilitate the electrolyte penetration. 3) the Co_3O_4 nanosheet arrays directly grown on the CC can reduce the ions diffusion length and improve the electrical conductivity of the electrode, which are beneficial to fast charge/discharge rates. Meanwhile, the active materials directly grown on the CC, without ancillary materials of polymer binder and carbon black, enhance the energy density and power density of the total electrode.

In summary, a simple and scalable preparation approach of Co_3O_4 NSAs/CC has been developed via an electrodeposition route. As anode for Li-ion batteries, the unique architecture of Co_3O_4 NSAs/CC exhibited high capacity, excellent rate performance and cyclic stability. The enhanced electrochemical performance of Co_3O_4 NSAs/CC electrode can be attributed to the hierarchical porous electrode architecture, which not only restrains the volume expansion of Co_3O_4 nanoparticles, but also facilitates the electrolyte penetration and electron/ion transport. As expected, this preparation process of Co_3O_4 NSAs/CC can be extended to fabricate other flexible electrode for Li-ion batteries.

Experimental

Synthesis: The commercial CC was pretreated in Teflon-lined stainless steel autoclave with concentrated HNO_3–H_2O (1:5, v/v) solution at 120 ℃ for 2 h, then washed with acetone, alcohol and deionized water, respectively, and finally dried in vacuum. The electrodeposition experiments were carried out in a 15 Mm $Co(NO_3)_2$•$6H_2O$ aqueous solution. Cyclic voltammetry was performed using a potentiostatat the applied potential of -1.8 to -0.7 V (vs SCE) with sweep rate of 50 mV s^{-1} for 15 cycles at room temperature. After deposition, the film was washed by deionized water for three times and dried at 60 ℃. To obtain the desired crystalline phase the as-prepared thin films were calcined at 250°C for 2h with a heating rate of 2 ℃ min^{-1}. The mass of Co_3O_4 nanostructures were obtained by the weight difference before and after electrodeposition. The loading density of active material is calculated as 0.8 mg cm^{-2}.

Material Characterization: The phase of the samples was characterized by X-ray powder diffraction (XRD, Siemens D-5000) with Cu Kα (λ = 0.15418 nm). The morphologies of the samples were observed by field-emission scanning electron microscopy (FESEM, Hitachi S-4800) and transmission electron microscopy (TEM, JEOL-2010).

Electrochemical Characterization: The electrochemical properties of the samples were evaluated using CR2016-type coin cells. The Co_3O_4 NSAs/CC was directly used as the working electrode for cell assembly. Pure lithium foils were used as the counter electrodes. A Celgard polypropylene membrane was used as a separator. The electrolyte consisted of a solution of 1 M LiPF6 in ethylene carbonate–dimethyl carbonate–diethyl carbonate (1 : 1 : 1 by wt%). The cells were assembled in an argon-filled glovebox. The discharge and charge measurements were carried out by a Land BT2001 battery test system with the voltage range of 0.01–3.0 V at ambient temperature. The cyclic voltammogram (CV) experiments were measured at room temperature on an Arbin battery test system at a

scan rate of 0.5 mV s^{-1}. Electrochemical impedance spectroscopy (EIS) tests were performed on a CHI660c electrochemical workstation with an amplitude of 5 mV sinusoidal voltage in the frequency range of 100 kHz to 0.01 Hz.

Acknowledgements

This work was partly supported from the National Natural Science Foundation of China (Grant No. 21003041 and 21373081), the Specialized Research Fund for the Doctoral Program of Higher Education of China (Grant No.20120161110016), and the Hunan Provincial Natural Science Foundation of China (Grant No. 11JJ7004).

Notes and references

[a] *Key Laboratory for Micro-Nano Optoelectronic Devices of Ministry of Education, and State Key Laboratory for Chemo/Biosensing and Chemometrics, Hunan University, Changsha 410082, China*
[b] *State Key Laboratory for Powder Metallurgy, Central South University, Changsha 410083, China*
[1] *These authors contributed to the work eqully and should be regarded as co-first authors*
Fax: +86 731 84214505; Tel: +86 731 84214606; E-mail: lbchen@hnu.edu.cn

[1] J.F. Li, S.L. Xiong, Y.R. Liu, Z.C. Ju, Y.T. Qian, *Appl. Mater. Interfaces*, 2013, **5**, 981.
[2] F.F. Cao, X.L. Wu, S. Xin, Y.G. Guo, L.J. Wan, *J. Phys. Chem. C*, 2010, **114**, 10308.
[3] L.H. Zhuo, Y.Q. Wu, J. Ming, L.Y. Wang, Y.C. Yu, X.B. Zhang, F.Y. Zhao, *J. Mater. Chem.A*, 2013, **1**, 1148.
[4] X. Wang, X.L. Wu, Y.G. Guo, Y.T. Zhong, X.Q. Cao, Y. Ma, J.N. Yao, *Adv. Funct. Mate.* 2010, **20**, 1680.
[5] N. Yan, L. Hu, Y. Li, Y. Wang, H. Zhong, X.Y. Hu, X.K. Kong, Q.W. Chen, *J. Phys. Chem. C*, 2012, **116**, 7227.
[6] Y. Sharma, N. Sharma, G.V. S. Rao, B.V.R. Chowdari, *J. Power Sources*, 2007, 173, 495.
[7] Y.N. NuLia, P. Zhang, Z.P. Guo, H.K. Liu, J. Yang, *Electrochem. Solid-State Lett*. 2008, **11**, 5, A64.
[8] W. Luo, X.L. Hu, Y.M. Sun, Y.H. Huang, *J. Mater. Chem*., 2012, **22**, 8916.
[9] M.V. Reddy, B.C. Zhang, K.P. Loh, B.V.R. Chowdari, *CrystEngComm*, 2013, **15**, 3568.
[10] M.V. Reddy, B.C. Zhang, L.J. Nicholette, K.M. Zhang, B.V.R. Chowdaria, *Electrochemical and Solid State Letters*, 2011, **14**, A79.
[11] H.W. Shim, Y.H. Jin, S.D. Seo, S.H. Lee, D.W. Kim. *ACS Nano*, 2011, **5**, 443.
[12] S.W. Hwang, A. Umar, S.H. Kim, S.A. Al-Sayari, M. Abaker, A. Al-Hajry, A.M. Stephan, *Electrochimi. Acta*, 2011, **56**, 8534.
[13] X.H. Xia, J.P. Tu, J.Y. Xiang, X.H. Huang, X.L. Wang, X.B. Zhao, *J. Power Sources*, 2010, **195**, 2014.
[14] C. Wang, D.L. Wang, Q.M. Wang, L. Wang, *Electrochimi. Acta*, 2010, **55**, 6420.
[15] D. Barreca, M.C. Yusta, A. Gasparotto, J. Morales, C. Maccato, A. Pozza, C. Sada, L. Sanchez, E. Tondello, *J. Phys. Chem. C*, 2010, **114**, 10054.
[16] M.V Reddy, G.V.S Rao, B. V. R. Chowdari, *Chemical Reviews*, 2013, **113**, 5364.
[17] C.C. Li, Q.L. Li, L.B. Chen, T.H. W, *J. Mater. Chem*, 2011, **21**, 11867.
[18] C.C. Li, X.M. Yin, L.B. Chen, Q.H. Li, T.H. Wang, *Appl. Phys. Lett*, 2010, **97**, 043501.
[19] S.L. Chou, J.Z. Wang, H.K. Liu, S.X. Dou, *J. Power Sources*, 2008, **182**, 359.
[20] H.C. Liu, S.K. Yen. *J. Power Sources*, 2007, **166**, 478.
[21] L.N. Gao, X.F. Wang, Z. Xie, W.F Song, L.J. Wang, X. Wu, F.Y. Qu, D. Chen, G.Z Shen, *J. Mater. Chem.A*, 2013, **1**, 7167.
[22] W.L. Yao, J. Yang, J.L. Wang, L. Tao, *Electrochimi. Acta*, 2008, **53**, 7326.
[23] J.k. Ryu, S.w. Kim, K. Kang, C.b. Park, *ACS Nano*, 2010, **4**,159.
[24] Y.F. Shi, B.K. Guo, S. A. Corr, Q.H. Shi, Y.H. Hu, K. R. Heier, L.Q. Chen, R. Seshadri, G. D. Stucky, *NanoLett*, 2009, **9**, 4215.
[25] J.G. Kang, Y.D. Ko, J.G. Park, D.W. Kim, *Nanoscale ResLett*, 2008, **3**, 390.
[26] Y. Liu, C.H. Mi, L.H. Su, X.G. Zhang, *Electrochimica Acta*, 2008, **53**, 2507.

